

**NASA TECHNICAL  
MEMORANDUM**

NASA TM X-67814

N 7 1 - 2 3 9 2 8

NASA TM X-67814

**CASE FILE  
COPY**

**EXPERIMENTAL EVALUATION OF THE ELECTRICAL SUBSYSTEM OF  
THE 2-TO-15 KW BRAYTON POWER CONVERSION SYSTEM**

by R. R. Secunde, J. E. Vrancik, and A. C. Spagnuolo  
Lewis Research Center  
Cleveland, Ohio

**TECHNICAL PAPER** proposed for presentation at 1971 Intersociety  
Energy Conversion Engineering Conference sponsored  
by the Society of Automotive Engineers  
Boston, Massachusetts, August 3-6, 1971

## ABSTRACT

The electrical subsystem of the 1200 hertz, 2-to-15 kilowatt Brayton Power Conversion System consists of the auxiliary electrical equipment required for an integrated, self-contained power conversion system. All of the electrical components with the exception of valve operators, heaters, and the turbine-compressor-alternator unit are included. These components are the speed controller, alternator voltage regulator, dc power supply, batteries, two inverters, two coolant loops including the 400 hertz motor-driven pumps, and the Brayton Engine Control System.

The electrical subsystem, powered by a motor-driven alternator, was evaluated under various system operating conditions in a vacuum environment in order to determine overall performance. A 10,000-hour endurance test in vacuum is underway to verify the ability of the subsystem to function properly during long-term operation in space.

Overall operation of the electrical subsystem was satisfactory. Deviations of system waveforms from a true sine wave have a small but measurable effect on the performance of individual components. Operation of the speed controller has a distorting effect on the 1200 hertz system voltage. The life of the originally selected silver-cadmium batteries was inadequate for long-term use in the Brayton power conversion system.

THE NASA, LEWIS RESEARCH CENTER, is investigating Brayton cycle electric power generating systems capable of operation in a space environment. This development has resulted in the design and construction of a complete power system capable of producing from 2-to-15 kilowatts, 1200 Hz, ac electrical power. The speed of the turbine-driven alternator and, thereby, the frequency of the generated ac power is maintained by a parasitic-loading speed controller which utilizes phase-delayed conduction in the power control stages.

As part of the overall Brayton-cycle system, the electrical subsystem provides the required regulation and control of the generated electrical power as well as control of the overall system. It also provides electric power for auxiliary system components such as the coolant pumps. Reference 1 describes the electrical subsystem and its performance as determined from early tests.

In this paper, we present the results of a program in which the performance of the overall electrical subsystem was experimentally evaluated under various system power conditions within the 2-to-15 kW range. Particular emphasis was placed on intercomponent compatibility-that is, how the performance of one component is affected by the simultaneous operation of other subsystem components. Also, this program is demonstrating the endurance of the Brayton electrical subsystem by a continuing life test in a vacuum environment.

These results, although obtained from the testing of a particular set of components, are indicative of the performance which might be expected of similar systems.

## DESCRIPTION OF ELECTRICAL SUBSYSTEM

The Brayton electrical subsystem is designed for space operation and consists of the alternator, the electrical control package (ECP), the parasitic load resistors (PLR), the dc power supply, two batteries, two inverters, and the Brayton control system (BCS).

For this evaluation, the two coolant pump-motor assemblies (PMA's) together with the cold plates and other coolant loop items required for the removal of heat from electrical subsystem components are considered parts of the electrical subsystem. Figure 1 shows a block diagram of the electrical subsystem.

The alternator is a turbine-driven, solid rotor machine. Its output power is generated at 1200 Hz, 3-phase, 120/208 volts.

The ECP contains the speed controller, the alternator voltage regulator, main load contactor, and current transformers for measurement of alternator and load currents. It also contains the power conversion circuits for the excitation of the alternator fields and several additional contactors used for system control.

The parasitic load resistors dissipate the excess power developed by the turbine-driven alternator. The amount of power diverted to the FLR is controlled by the speed controller in the ECP so that the total load on the alternator is maintained relatively constant regardless of user (vehicle) load. The speed controller, together with the FLR, has three three-phase channels. Each channel is rated at 6 kW. The control of the power in these channels is by means of phase-delayed conduction of silicon controlled rectifiers in a bilateral connection. The channels are energized sequentially with increasing frequency. Reference 2 describes the functioning of the speed controller, FLR, and voltage regulator in more detail.

The dc power supply converts ac power from the alternator to + and -30 volts dc to supply the electrical subsystem components. It is a polyphase, unregulated, transformer-rectifier type device without output filters. The dc power supply also contains battery chargers and stepping-motor, ampere-hour type circuits for measuring and indicating battery state of charge. Changeover of the dc busses from alternator-supplied power to battery power is automatic on loss of alternator power or failure of the transformer rectifier. Manual override controls are also provided.

The two batteries are included in the subsystem to provide dc power for subsystem operation during Brayton system startup and shutdown, and for short term backup power in the event of transformer-rectifier or alternator malfunction.

The Brayton power system uses two coolant loops to provide redundancy for component cooling. The electrical subsystem components are mounted on four dual-path cold plates connected in series. The coolant fluid is dimethyl polysiloxane (Dow Corning type DC-200). Normally, one loop operates while the other serves as a standby. Each loop is independent and complete with a separate pump. The inverters convert power from the + and - 30-volt dc busses (60V) to 400 Hz, 3-phase ac power for driving the induction motors of the pump-motor-assemblies (PMA's). These inverters do not have output transformers,

and provide a nominal output voltage of 47 volts rms, line-to-line. The output waveform is a quasi-square wave. The inverters are permanently connected to the dc busses and to the PMA's. Start and stop control is obtained by furnishing a pulse to control circuits internal to the inverters. An experimental evaluation of the pump is reported in Ref. 3, and of the inverters in Ref. 4.

The Brayton control system (BCS) provides the necessary control and monitoring for overall Brayton power system operation. It consists of two major assemblies, a signal conditioner and a control and monitoring console. The signal conditioner is designed for space environment and is located with the Brayton power system. The control and monitoring console is designed for operation with convection cooling in a shirt-sleeve environment. Its circuits, however, were designed for ready adaptation to a space environment. The signal conditioner accepts power system instrumentation and logic signals and converts them to 0-5 volt signals for transmission to the control console. It also acts as the interface for control commands originating at the control console. The present system uses a multi-conductor, wire link between the signal conditioner and the control and monitoring console. The design is such, however, that a telemetry link could be used. The BCS is described fully in Ref. 5.

#### EXPERIMENTAL APPROACH

**BRAYTON AND SUPPORT EQUIPMENT** - The Brayton electrical subsystem, less the alternator, was assembled on a frame as shown in Fig. 2. This simulates the actual Brayton system assembly as described in Ref. 1. For all evaluations discussed in this paper, the Brayton alternator was simulated with a variable-frequency motor-driven alternator. The dynamic output impedances of the motor-driven alternator are approximately the same as those of the Brayton alternator. This simulation allows a high degree of flexibility in test conditions. The subsystem as shown in Fig. 2 is operable both inside a 6-foot (1.8-m) diameter vacuum tank as well as in a room environment. The variable-frequency alternator is located external to the tank. Also, for flexibility, power to individual Brayton components can be disconnected by remotely controlled latching relays. Auxiliary power sources and loads are available to allow most components to be operated independently.

In order to be completely functional, the Brayton control system requires input signals from temperature, flow, pressure, and other transducers located on Brayton components which are not a part of the electrical subsystem. Such inputs come from the gas heat exchanger, turbine, etc. All control functions which are operated by the BCS are within the electrical subsystem with the exception of electrically operated valves. The inputs to the BCS which are not available from the electrical subsystem are simulated with electrical signals. The electrically-operated valves are simulated with relays. This simulation equipment is located external to the vacuum tank. Also, the Brayton alternator fields (series and shunt) are simulated with a dual-winding reactor which provides loads for the alternator excitation circuits in the ECP.

All power, load, control, simulation, and instrumentation leads are brought through the vacuum tank bulkhead in connector-type feed-throughs.

**DATA ACQUISITION** - The bulk of performance data was taken and partially reduced by a computer-controlled automatic data acquisition system. This system is similar to that described in Ref. 6. It contains a DEC PDP8/I computer, a teletype, two reed-relay scanners, two digital voltmeters (one dc and one ac true rms), a digital clock, and a special high-frequency wattmeter. The wattmeter was developed at Lewis Research Center and is described fully in Ref. 7.

In each data scan, a total of 219 parameters were measured, converted to engineering units, and printed. All ac voltage and current measurements were taken with the true rms digital voltmeter. The response time of this meter is approximately four seconds. Since 43 ac measurements were included in each data scan, the scan was spread over an interval of three and one-half minutes. Along with controlling the acquisition and conversion of this data, the computer made certain calculations. It computed and recorded volt-amperes, total ac power, power factors, dc power, and component efficiencies.

In addition to performing some of the obvious data reduction, the data acquisition system prints out the measured and computed parameters in a logical and clear format. This facilitates finding a particular piece of data for future study or reduction. A section of the data print-out is shown in Fig. 3.

In addition to the data collected by the data acquisition system, waveform data was obtained with a wave analyzer and a distortion

meter. A digital counter was used to accurately measure the system frequency. The automatic data system also measures frequency but uses a frequency-to-dc converter. The expected 0.5 percent accuracy in the frequency-to-dc conversion produces a 6 Hz error in the 1200-Hz range. This amount of error is not tolerable when describing some aspects of electrical subsystem performance, such as speed controller operation.

**TEST PROCEDURE** - In order to determine their performance, the individual Brayton components were operated from auxiliary power sources and with simulated loads where necessary.

It was expected that phase-delayed conduction in the power stages of the parasitic-loading speed controller would have significant effects on the system voltages and currents. The operation of a transformer-rectifier dc supply in a small ac system causes a small, but noticeable, distortion in the system ac voltage. Also, the dc bus voltage contains a significant ripple component (1)\*. In order to determine the effects of voltage distortion, harmonic currents, ripple voltages, etc. on overall performance, the electrical subsystem was operated under various combinations of total system power, and parasitic load power.

The overall system power levels used (power delivered by the alternator) were 5, 10, 12, and 15 kW. It was assumed that the net power factor (PF) of the user load would be 0.8. The various user loads were applied to the system with a resistive-reactive load bank. For each user load setting, the system frequency was manually varied until the speed controller applied the amount of parasitic load necessary to bring the power drawn from the alternator to the desired level, i.e., 5, 10, 12, or 15 kW. The power to operate the electrical subsystem was included in total system power. Under these conditions, data were taken and reduced to show the variations in losses, efficiency, distortion, neutral currents, etc.

The power drawn by the Brayton control system from the dc bus varies in magnitude because of the small thermocouple ovens which it contains. This cycling is approximately + and - 7 percent of the BCS average power. For the parts of this evaluation where efficiency and losses were determined, the BCS load on the dc bus was simulated with a constant load equal to the BCS average.

\*Numbers in parentheses designate References at end of paper.

To simulate a space environment and to allow evaluation of the effectiveness of the coolant loops, the electrical subsystem was operated in the vacuum tank for the evaluation described in this paper. The pressure in the tank was maintained at less than  $1 \times 10^{-5}$  torr ( $1.33 \times 10^{-3}$  N/m<sup>2</sup>), and the shroud walls of the tank were maintained at 10° C. Also, the system was operated with both -46° C and +50° C vacuum tank shroud wall temperatures to determine the effects of these temperatures on subsystem heat rejection. The temperature of the DC-200 coolant into the Brayton cold plates was maintained at 20° C, which is the design value for this temperature in the Brayton system.

Subsystem component temperatures as well as the temperature of critical parts within the components were monitored during all test conditions. Where large changes in temperature were observed, the test condition was maintained and data was taken after those changes were within 10 percent of their final value. An exception to this practice was made if it appeared that a particular temperature might exceed a safe limit.

The endurance of the Brayton electrical subsystem is being demonstrated by nearly continuous operation in a vacuum. Various system power levels between 2 and 15 kW are used. The endurance test is interrupted only for detail performance tests and the incorporation and evaluation of subsystem improvements. For the endurance demonstration, the test facility operates unattended. Routine data acquisition, limit checking, and minor test control are performed by the computer-controlled data system. Sufficient protective measures have been incorporated into the facility to allow a safe shutdown in the event of a facility or electrical subsystem malfunction.

## DISCUSSION OF RESULTS

When an alternator is supplying a linear load, the load voltage waveshape is generally that produced by the alternator; however, when non-linear elements such as controlled rectifiers or common rectifiers are also connected to the load bus, the load voltage will be distorted. The degree of distortion will depend on the nature and magnitude of the non-linear load and the alternator commutating leakage reactance. In the Brayton alternator these reactances are in the order of 0.8 ohm. The motor-driven alternator used in this program to simulate the Brayton alternator has a similar reactance value in the

order of 0.9 ohm. These values were determined from the phase conduction overlap existing when a polyphase rectified load was connected to the alternators. Therefore, the effects on alternator and load voltage as determined with the motor-driven alternator in this program will approximate those which exist with the Brayton alternator.

**OPTIMUM OPERATION** - In the Brayton power system the user load voltage is affected by the normal operation of the power system. In order to provide a reference so that the effects of electrical subsystem operation can be better appreciated, the user load voltage wave form with the Brayton dc power supply disconnected and the speed controller fully off is shown in Fig. 4. This voltage wave form was obtained with the user load set at 10 kW 0.8 PF and with the voltage at the system rating of 120/208 volts. The total distortion is approximately 2.0 percent and consists almost solely of the fifth harmonic.

Capacitors are used in the ECP for preventing high-frequency electrical noise generated by the speed controller from reaching the user load terminals. These capacitors are connected to the ac voltage lines and present a leading power factor load of approximately 2 KVAR to the alternator. As a result of this leading power factor load, the net alternator power factor was 0.9, lagging, in the reference test.

**DC POWER SUPPLY PERFORMANCE** - The dc power supply provides approximately 940 watts for steady-state subsystem operation. During steady-state operation, the batteries are not being charged or discharged. Transformer-rectifier circuits in the dc power supply convert ac power from the system to + and - 30 volts dc. The effect of dc supply operation on the user-load wave shape is shown in Fig. 5. This wave shape exists with steady-state subsystem operation with the speed controller fully off. The effect is very small, being the slight notching or apparent discontinuities, in the wave form. There is also an increase in the third harmonic component and a reduction in the fifth. The total distortion remained at approximately 2 percent with approximately equal magnitudes of the third and fifth harmonics. The notching is the result of rectifier commutation, and the presence of the third harmonic is a result of the non-linear input impedance of the transformers.

In normal system operation, the load on the dc supply is not balanced between the + and - 30 volt lines. The inverters are a balanced load, but the BCS power is approximately 0.32 kW

from the + line and 0.08 kW from the - line. The net power load on the dc supply is approximately 0.59 kW on the + line and 0.35 kW on the - line.

The operation of the dc supply introduces a neutral current into the system. The rms value of this current is approximately two amperes, and its wave form is shown in Fig. 6. The predominant frequency of this current is the third harmonic, the magnitude of which is approximately 160 percent of the fundamental (the fundamental being 1200 Hz). The total harmonic content is 178 percent of the fundamental.

The efficiency of the dc supply when providing dc power for all subsystem steady-state functions is approximately 88 percent. The dc output voltage is unfiltered and contains a ripple component which varies in magnitude depending on the amount of distortion in the system ac voltage. The minimum ripple on the 30 volt bus observed in this evaluation was approximately six volts peak-to-peak. This minimum occurred with the speed controller operation inhibited completely. The predominant ripple frequency is 14.4 kilohertz as would be expected with the 12-phase type rectifier circuit used.

**INVERTER PERFORMANCE** - The inverter provides approximately 415 watts of 400 Hz, 3-phase ac power for the operation of the coolant pumps. The input power is obtained from the + and - dc busses as a two-wire input giving an inverter nominal input voltage of 60 volts. The inverter has input filters to provide high-frequency isolation between the inverter circuits and the rest of the subsystem.

The efficiency of the inverters when driving the coolant pumps at normal conditions of 3.18 gal/min ( $1.2 \times 10^{-2} \text{ m}^3/\text{min}$ ) with a pressure rise of approximately 70 psi ( $48 \text{ N/cm}^2$ ) is 77 percent. Reference 4 provides additional inverter performance data. The ripple on the dc bus in the fully-functioning electrical subsystem is not transmitted through the inverter to the inverter ac output voltage and had no noticeable effect on normal inverter performance.

**SPEED CONTROLLER OPERATION** - As the speed controller changes parasitic load in response to varying user loads, the effects of the phase-delayed conduction in the speed controller power stages will vary. The operation of the Brayton speed controller and its effects on the Brayton alternator currents are fully described in Ref. 2. In this paper we will describe the effects of speed controller operation on the electrical subsystem and the net effects of speed

controller and subsystem operation on user load voltage.

Pictorial examples of the effect of phase-delayed conduction in the parasitic load on the wave form of the user voltage are shown in Fig. 7.

The wave shapes of Fig. 7(a) are representative of those obtained at the 5 kW system power level. Those of Figs. 7(b) and 7(c) were obtained at the 10 and 15 kW power levels. The actual shape is quite variable with parasitic load; therefore, the total distortion in user voltage wave shape, as measured with the distortion meter, is plotted in Fig. 8 as a function of parasitic load power. Although the data have some scatter, the general trend is evident. The minimum distortion of approximately 3 percent occurs at minimum parasitic load. The maximum measured distortion of between 12 and 14 percent occurs near 4 kW and 13 kW parasitic loads. These distortions are the net effect of the parasitic load, user load, and electrical subsystem loads.

The data in Figs. 7 and 8 for the 10 kW system power level are similar to those presented in Ref. 2. The data at the 5, 12, and 15 kW system power levels provide additional information to describe the performance of the electrical subsystem over the range of power of which the Brayton power system is capable.

The electrical subsystem is an approximately constant power load of about 1.1 kW on the alternator if the parasitic load and alternator field load are not included. The dc power supply which represents the major subsystem load has an input power factor of about 0.89 lagging. The effective power factor of the parasitic load varies as shown in Fig. 9. The phase-delayed conduction is similar in effect to a reactive component in the load. This is explained more fully in Refs. 8 and 9. Power factor as used in this paper is defined as kW/kVA or the ratio of real power to the product of rms volts and rms amperes. The net power factor as seen by the alternator in this electrical subsystem is shown as a function of parasitic load in Fig. 10. The data in this figure were obtained with the user load PF at 0.8. As the figure shows, the power factor of the net load on the alternator is relatively independent of system power level and always higher than the power factor of the user load. This is the result of the high power factor of the dc supply and the capacitors in the ECP. These offset the low power factor of the parasitic load at low parasitic load values.

The result of a subtraction of user load

power, alternator field power, and parasitic load power (as applied by the speed controller) from the alternator output power is the net electrical subsystem power loss. This power loss has also been termed "housekeeping power." Because of the voltage distortion and the existence of harmonic components in both voltages and currents, the net electrical subsystem loss varies with parasitic load power. This variation is shown in Fig. 11. The losses are generally higher at the 15 kW system power levels because of the greater power required by the alternator fields and the increased losses in the power handling components in the ECP. The total system loss generally tends to be a maximum around 4 to 8 kW of parasitic load. This is probably the result of the effects of harmonic currents and voltages. These losses were further evidenced by a significant increase in the temperature of the alternator field supply current transformers located in the ECP. This increase in temperature occurs around the 4 kW parasitic load condition. The maximum distortion on the user load voltage also occurs at this condition, which would indicate that the harmonic currents cause additional losses. The data in Fig. 11 show a fairly large degree of scatter and should, therefore, be taken only as indicative of general levels and trends.

The variation in distortion of the system ac voltage is transferred through the dc power supply to the dc bus as a variation in ripple. The system voltage distortion also has a small effect on the efficiency of the dc power supply. Fig. 12 shows the variation in dc bus voltage ripple and dc power supply efficiency as functions of parasitic load. The ripple generally is minimum at zero parasitic load. The minimum shown on Fig. 12 is approximately two volts higher than the minimum obtained with the speed control circuit inhibited. This is a result of the fact that the parasitic loads shown in Fig. 12 were not truly zero, but in the order of 50 to 100 watts, and so caused a slight distortion in the system ac voltage. The maximum ripple observed was approximately 18 volts peak-to-peak on the +30 volt bus. The parasitic load at which maximum ripple will occur is difficult to predict since the ripple is the net effect of the rectifier circuit used and the ac voltage wave shape.

Unbalanced conduction in the parasitic load phases and induced transient spikes further complicate such a prediction. There is little change in dc supply efficiency as the parasitic load changes, but it does show a tendency to drop when the parasitic load is between 2 and 4 kW. A

parasitic load of this value requires one channel of the speed controller to function with the phase delayed conduction beginning around  $90^\circ$ .

The phase-delayed conduction of the parasitic load causes a current to exist in the neutral of the alternator. The magnitude of this current and its variation with parasitic load are discussed in Ref. 2. The frequency of this current is approximately 3600 Hz or the third harmonic of the frequency of the system voltage. The maximum value of neutral current observed in this subsystem evaluation was 18.1 amperes with a 15 kW system power and a parasitic load of 13.7 kW. The user load was zero. This value of neutral current is the net result of neutral current from the dc supply and from the parasitic load. These two neutral currents are not in phase, and add vectorially. At this load condition, the parasitic load neutral current was approximately 16.4 amperes and the dc supply neutral current was approximately 3.0 amperes. At a 10 kW system power level, the maximum observed alternator neutral current was 13.2 amperes which occurred with a parasitic load of 3 kW.

**SEPARATION OF SUBSYSTEM LOSSES** - The power dissipated by the various subsystem components varies with system operating conditions as described in preceding sections of this paper. The nominal power lost in the various subsystem components under a typical operating condition is given in Table I.

**HEAT REJECTION FROM ELECTRICAL SUBSYSTEM** - The parasitic load is designed to dissipate its heat to space by direct radiation. In this evaluation, it radiated to the vacuum tank shroud walls which were maintained at a relatively constant temperature of  $+10^\circ\text{C}$ . At this shroud temperature, the maximum observed temperature on a parasitic load element was  $637^\circ\text{C}$ . This occurred with a 15 kW system power level and 13.7 kW parasitic load. At a 10 kW system power level and 8.75 kW parasitic load the maximum load element temperature was  $617^\circ\text{C}$ . The design temperature for these load elements was approximately  $700^\circ\text{C}$ .

The Brayton coolant pumps are self-cooled by the DC-200 coolant fluid which is circulated through the motor (see (3)). Heat is removed from the remaining electrical subsystem components through the cold plates on which they are mounted. At normal operating conditions and 10 kW system power, the DC-200 coolant enters the first cold plate at  $20^\circ\text{C}$  and exits the fourth (last) cold plate at  $29^\circ\text{C}$ . The flow is maintained at 0.58 gal/min ( $2.2 \times 10^{-3} \text{ m}^3/\text{min}$ ). The total heat

removed from the cold plates by the coolant is, therefore, approximately 490 watts. This heat removal is approximately constant for all system power levels. The sink or surrounding shroud wall temperature, however, has an effect on the coolant temperature. The above results were obtained with the sink temperature at  $+10^{\circ}\text{C}$ . To investigate the effect of sink temperature, the electrical subsystem was also operated with the shroud walls at  $+50^{\circ}\text{C}$  and  $-46^{\circ}\text{C}$ . System power was maintained at 10 kW. At  $+50^{\circ}\text{C}$  sink temperature, the cold plates picked up heat from the sink and the total heat removed from them by the coolant was found to be approximately 870 watts. At  $-46^{\circ}\text{C}$  sink temperature, the cold plates gave up heat to the sink and the total heat removed from them by the coolant was approximately 57 watts. The measured electrical losses to the cold plates remained approximately constant at 530 watts for all sink temperatures.

**ENDURANCE TEST RESULTS** - The electrical subsystem has been in nearly continuous, unattended operation since November 1970 in a vacuum environment in the facility described in this paper. It has been operating at various power levels with various amounts of power dissipated by the parasitic load elements.

The batteries originally used in the subsystem were of a sealed, AgCd type with an 85 A-hr rating. These batteries failed after several cycles during the checkout phase of this program. Failure was caused by silver penetration through the separators. The failures occurred approximately 1.5 to 2 years after manufacture of the cells. Prior to operation in the subsystem, the batteries had been stored at room temperature in an undetermined state of charge. A study to determine the most suitable batteries for this subsystem is now underway. The subsystem is being operated with simulated batteries until the final batteries are available.

With the exception of the battery failures and several minor, non-critical failures in the monitoring functions of the Brayton control system, there have been no significant problems experienced with the operation of the Brayton electrical subsystem.

As of March 23, 1971, 3,938 hours of subsystem operation have been accumulated. Of these hours, 3,717 were in an unattended mode.

It is presently planned to continue the endurance test to 10,000 and possibly 20,000 hours.

Also, as of the above date, separate endurance tests have demonstrated satisfactory operation of an inverter-coolant pump combination for

12,250 hours, and of a Brayton dc power supply for 14,700 hours.

#### CONCLUDING REMARKS

The operation of the phase-delayed conduction, parasitic-loading speed controller induces a 3 to 14 percent distortion into the waveform of the voltage supplied by the electrical subsystem for user loads. The speed controller operation also has a small, but noticeable, effect on the performance of other subsystem components. Subsystem losses, alternator power factor, neutral current, and dc bus voltage ripple vary with the amount of parasitic load. Interactions among subsystem components are small but should be considered in the design and application of an electrical power generating system of this type.

The performance evaluation and endurance testing of a prototype electrical subsystem for the 2-to-15 kW Brayton power system has demonstrated that the subsystem should be capable of satisfactory, long-term performance in a vacuum environment.

#### REFERENCES

1. P. A. Thollot, R. C. Bainbridge and J. Nestor, "Description and Performance of the Electrical Subsystem for a 2-to-15 kW Brayton Power System." Intersociety Energy Conversion Engineering Conference, AIAA, Las Vegas, Nevada, September 1970.
2. B. D. Ingle, H. L. Wimmer and R. C. Bainbridge, "Steady-state Characteristics of a Voltage Regulator and a Parasitic Speed Controller on a 14.3 Kilovolt-Ampere, 1200-Hertz Modified Lundell Alternator." NASA TN D-5924, November 1970.
3. A. C. Spagnuolo, R. R. Secunde and J. E. Vrancik, "Performance of a Hermetic Induction Motor-Driven Pump for Brayton Cycle Heat Rejection Loop." NASA TM X-52698, October 1969.
4. A. G. Birchenough and R. R. Secunde, "Performance Evaluation of Brayton Space Power System 400-Hertz Inverters." NASA TM X-2141, December 1970.
5. R. L. Thomas, R. S. Bilski and R. A. Wolf, "Requirements, Design, and Performance of a Control System for a Brayton Power System." Intersociety Energy Conversion Engineering Conference, AIAA, Las Vegas, Nevada, September 1970.



6. R. A. Edkin and R. P. Macosko, "Experience with Automated Endurance Testing a Brayton Power Conversion System." Paper to be presented at this Conference (IECEC 1971).
7. J. E. Vrancik, "Design and Performance of a High-Frequency Wattage-to-Voltage Converter." NASA TN D-5674, February 1970.
8. L. J. Gilbert, "Reduction of Apparent-Power Requirement of Phase-Controlled Parasitically-Loaded Turboalternator by Multiple Parasitic Loads." NASA TN D-4302, February 1968.
9. D. A. Perz and M. E. Valgora, "Experimental Evaluation of Volt-Ampere Loading and Output Distortion for a Turboalternator with Multiple Load Phase-Controlled Parasitic Speed Controller." NASA TN D-5603, December 1969.

Table 1 - Subsystem Component Losses at Nominal 10 kW System Power

Alternator Power (kW)	10.22
User Load Power (kW, 0.8 PF)	6.07
Parasitic Load (kW)	3.03
Alternator Fields (Simulated Fields) (kW)	0.03
<hr/>	
Losses (kW)	
ECP Loss	0.03
dc Supply Loss	0.12
Inverter Loss	0.12
BCS Power	0.40±.03
Pump Power	<u>0.42</u>
Total Subsystem Loss	1.09±.03

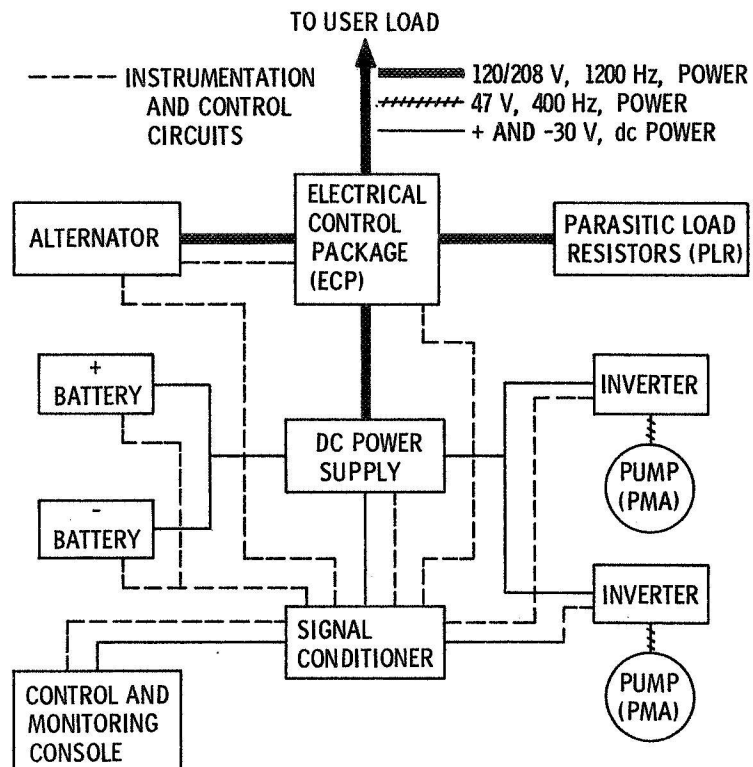


Figure 1. - Brayton electrical subsystem block diagram.

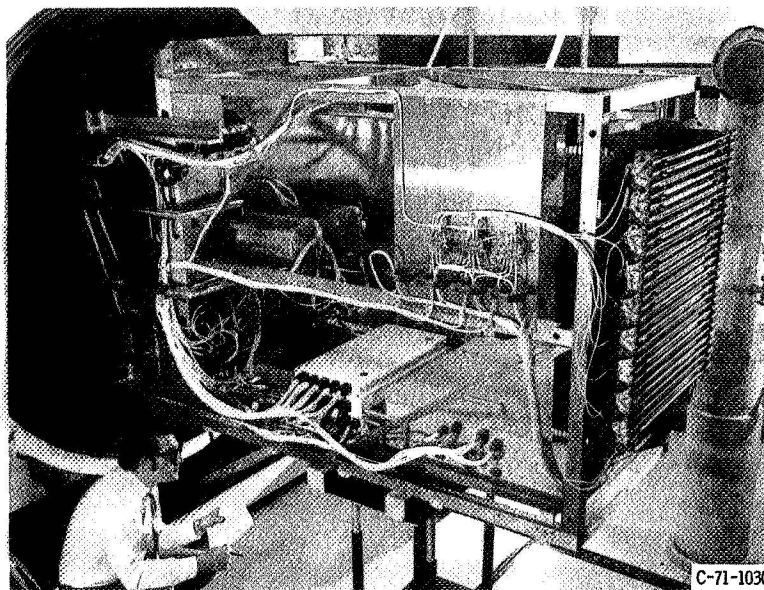


Figure 2. - Electrical subsystem evaluation assembly.

BRAYTON TEST CW19 069:14:25:23

ALT OUT

	V	I	PWR	VA
A	119.2840	31.2500	A 3287.4800	A 3727.6000
B	121.5200	30.7500	B 3298.9300	B 3736.7200
C	120.0580	32.1099	C 3433.4000	C 3855.0300
		N 3.1800	TOT 10019.800	TOT 11319.300

PF 0.8852

FREQ-1204.5200

VEHIC LOAD IN

	V	I	PWR	VA
A	118.7680	30.8599	A 2961.9500	A 3665.1500
B	120.9180	30.3399	B 2939.9400	B 3668.6300
C	119.1980	31.0499	C 2987.4100	C 3701.0700
		N 1.2600	TOT 8889.3000	TOT 11034.900

PF 0.8056

DC SUPPLY IN

	V	I	PWR	VA
A	119.8850	2.9420	A 314.8930	A 352.7020
B	121.9500	3.0360	B 312.5990	B 370.2380
C	120.1440	3.7340	C 403.2760	C 448.6140
		N 2.1680	TOT 1030.7700	TOT 1171.5500

PF 0.8798

INV A OUT

	V	I	PWR	VA
A	28.0880	8.5060	A 136.0330	A 238.9150
B	28.1826			
C	28.3202			
			TOT 408.0970	TOT 716.7450

PF 0.5694

DC SUPPLY OUT

	V	I	PWR
+B	30.2199	+I 18.7800	+B 567.5290
-B-	30.3999	-I- 11.2700	-B 342.6070
		N 5.9200	TOT 910.1350

INV. A IN

	V	I	PWR
+B	30.2199	+I 8.8200	+B 266.5390
-B-	30.3999	-I- 8.8200	-B 268.1270
			TOT 534.6660

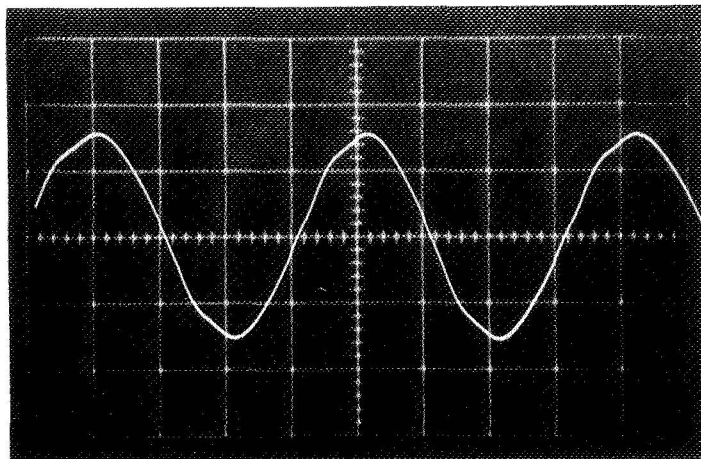
INV. B IN

	V	I	PWR
+B	30.2199	+I 0.0050	+B 0.1511
-B-	30.3999	-I- 0.0400	-B 1.2160
			TOT 1.3671

SIG. COND. IN

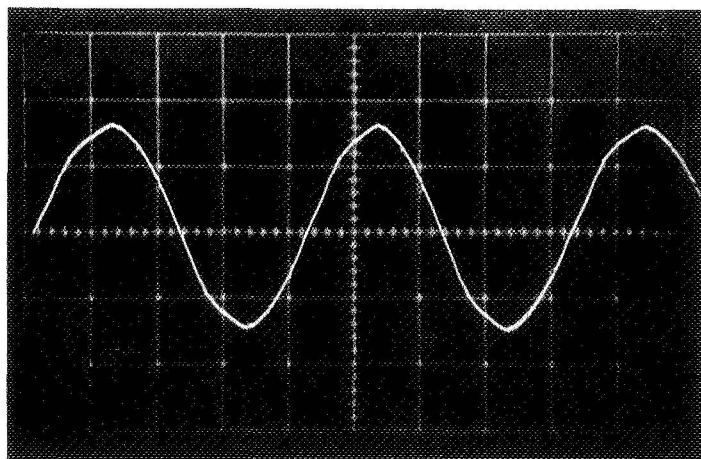
	V	I	PWR
+B	30.2199	+I 9.7450	+B 294.4920
-B-	30.3999	-I- 2.4650	-B 74.9358
		N 5.6900	TOT 369.4280

Figure 3. - Typical printout from automatic data system.



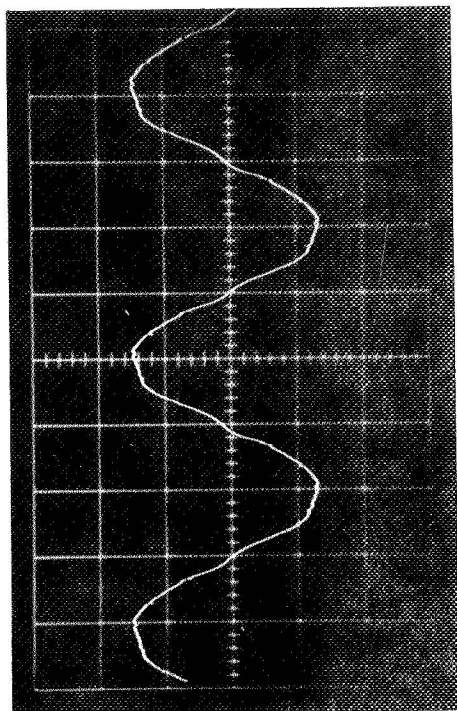
10 kW, 0.8 PF USER LOAD  
 DISTORTION: 2.0 PERCENT  
 PREDOMINANT HARMONIC: 5TH

Figure 4. - User load voltage wave shape without dc supply or parasitic loads (1200 Hz).

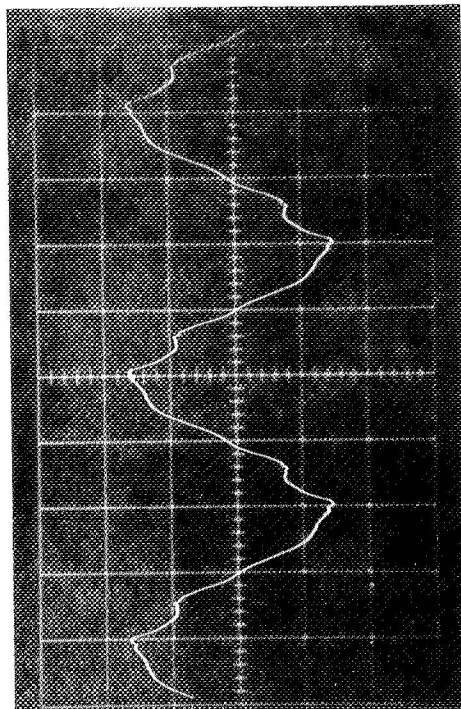


10 kW SYSTEM; 9 kW, 0.8 PF USER LOAD  
 DISTORTION: 2.0 PERCENT  
 PREDOMINANT HARMONICS: 3RD & 5TH

Figure 5. - User voltage wave shape as effected by normal dc supply operation in subsystem (1203 Hz).

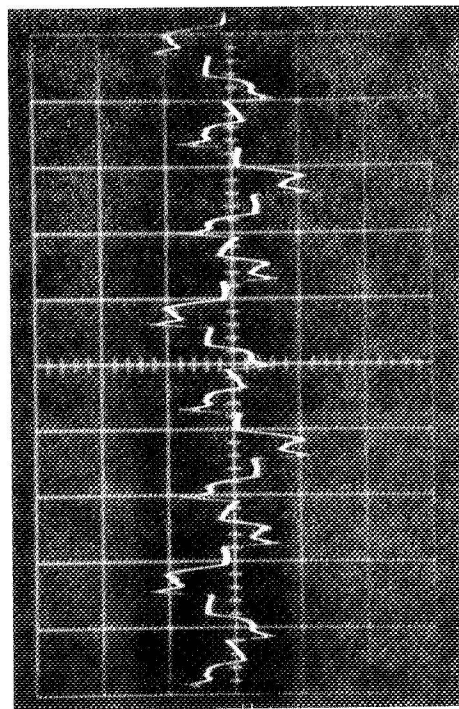


0.04 kW PARASITIC LOAD (1204 Hz)  
DISTORTION: 4.1 PERCENT  
PREDOMINANT HARMONICS: 5TH & 7TH



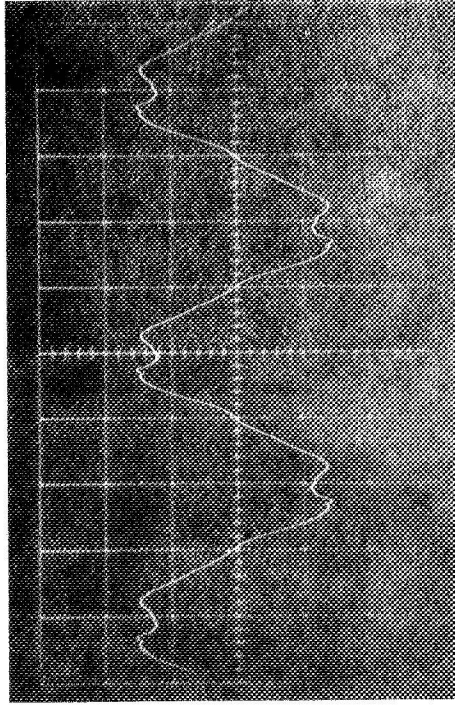
1.8 kW PARASITIC LOAD (1214 Hz)  
DISTORTION: 9.2 PERCENT  
PREDOMINANT HARMONICS 3RD, 5TH, & 7TH

Figure 7(a). - User voltage wave shapes, 5 kW system power.

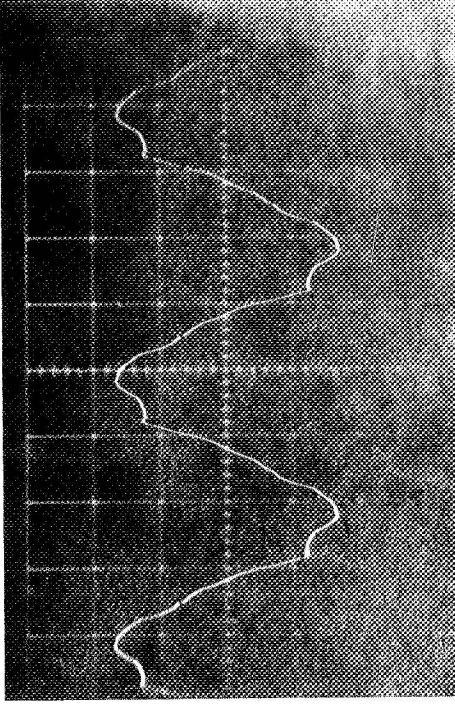


PREDOMINANT FREQUENCY: 3600 Hz  
TOTAL HARMONIC CONTENT: 178 PERCENT OF 1200 Hz COMPONENT  
rms VALUE: 2.0 AMPERES

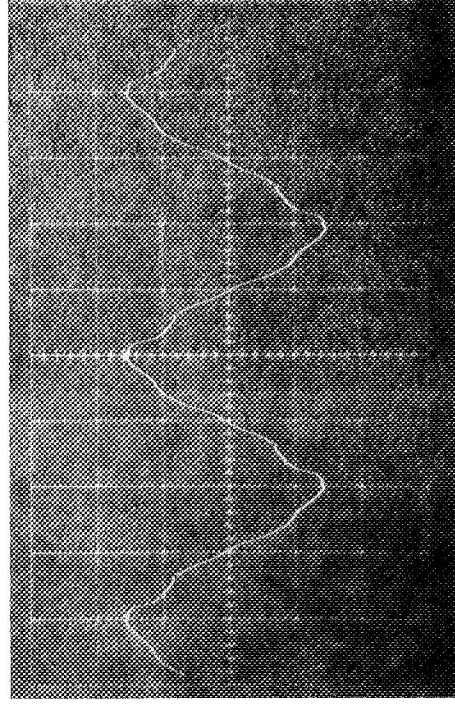
Figure 6. - dc Supply neutral current wave form.



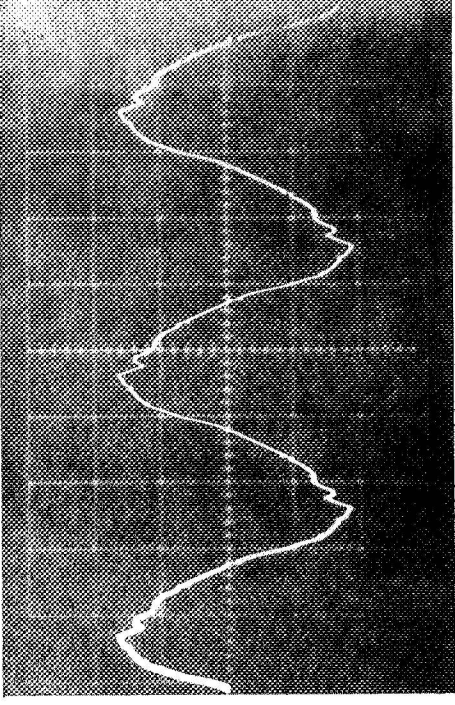
4.3 kW PARASITIC LOAD (1222 Hz)  
DISTORTION: 11.0 PERCENT  
PREDOMINANT HARMONICS: 3RD & 5TH



6.3 kW PARASITIC LOAD (1227 Hz)  
DISTORTION: 9.0 PERCENT  
PREDOMINANT HARMONIC: 5TH



7.5 kW PARASITIC LOAD (1230 Hz)  
DISTORTION: 8.0 PERCENT  
PREDOMINANT HARMONICS: 3RD & 5TH



11.3 kW PARASITIC LOAD (1241 Hz)  
DISTORTION: 11.0 PERCENT  
PREDOMINANT HARMONIC: 3RD

Figure 7(b). - User voltage wave shapes, 10 kW system power.

Figure 7(c). - User voltage wave shapes, 15 kW system power.

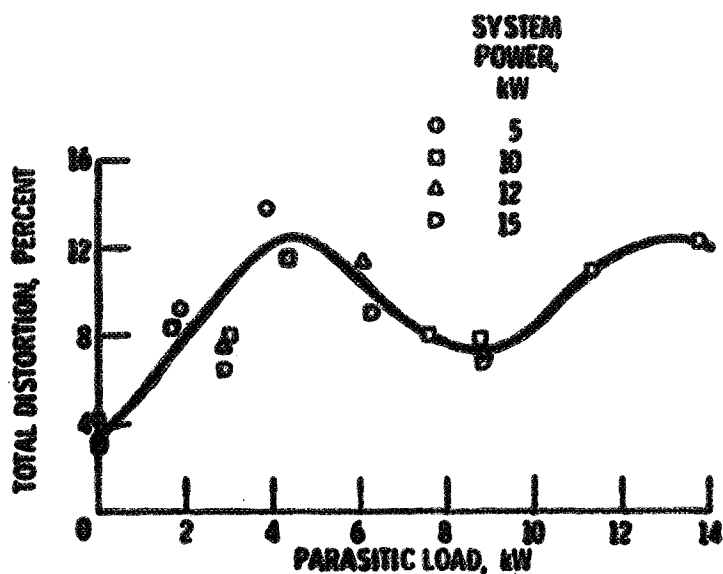


Figure 8. - User load voltage total distortion as a function of parasitic load.

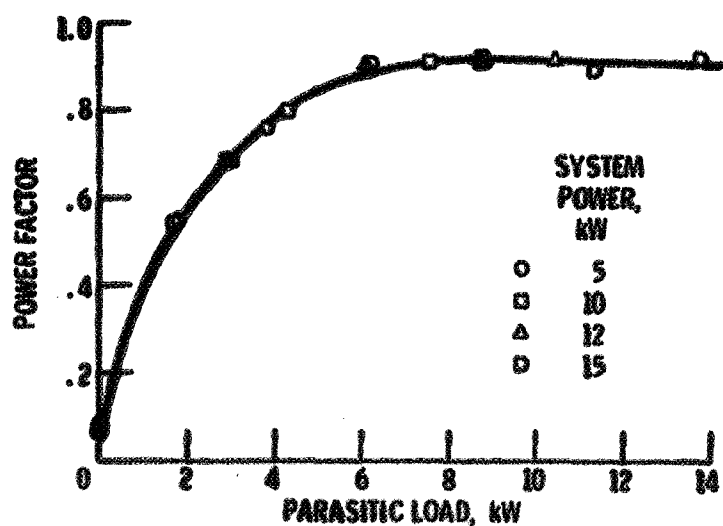


Figure 9. - Parasitic load power factor as a function of parasitic load.

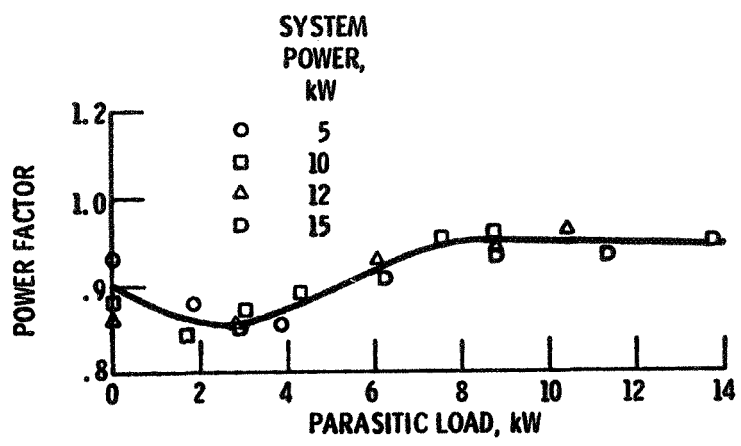


Figure 10. - Alternator power factor as a function of parasitic load.

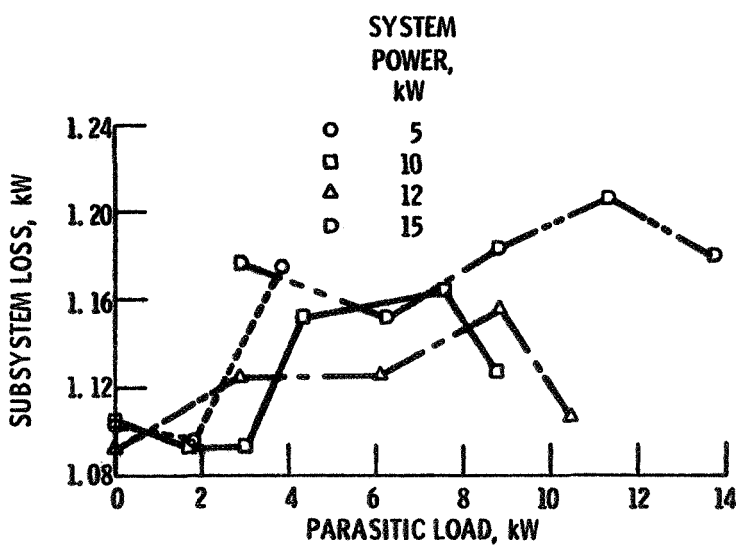


Figure 11. - Electrical subsystem loss as a function of parasitic load.



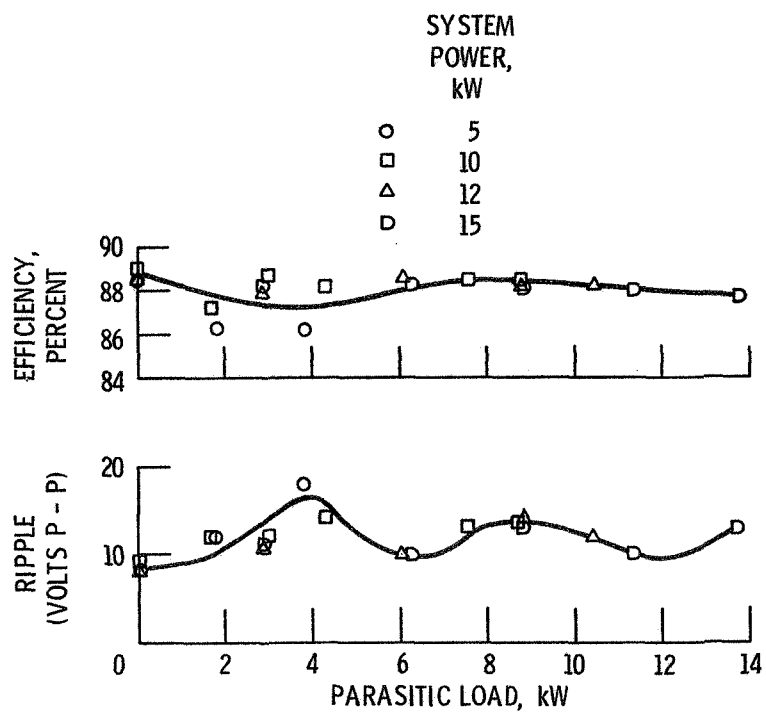


Figure 12. - DC power supply efficiency and output voltage ripple as a function of parasitic load.